

Responsive MR-imaging probes for *N*-methyl-D-aspartate receptors and direct visualisation of the cell-surface receptors by optical microscopy†

Cite this: *Chem. Sci.*, 2013, **4**, 3148

Neil Sim,^a Sven Gottschalk,^{‡b} Robert Pal,^a Jörn Engelmann,^b David Parker^{*a} and Anurag Mishra^{‡*a}

Received 4th April 2013

Accepted 5th June 2013

DOI: 10.1039/c3sc50903f

www.rsc.org/chemicalscience

A series of *N*-methyl-D-aspartate (NMDA) receptor-targeted MRI contrast agents has been developed, based on the known competitive NMDA antagonist, 3,4-diamino-3-cyclobutene-1,2-dione. Their use as responsive MR imaging probes has been evaluated *in vitro* and two contrast agents showed 170–176% enhancements in relaxation rate, following incubation with a neuronal cell line model. A derivative of the lead compound was prepared containing a biotin moiety, and both the specificity and reversibility of binding to the NMDA cell surface receptors demonstrated using confocal microscopy.

Introduction

Glutamate receptor proteins are classed into two main families, the ligand-gated ionotropic receptors (iGluRs) and the G-protein-coupled metabotropic receptors (mGluRs); each of these is further branched into three subclasses. The NMDA receptor (NMDAR) from the iGluR family has received growing interest over the past decade owing to its role in excitatory neurotransmission, synaptic plasticity, memory and learning.¹ Following activation of the NMDAR by glutamate and co-agonist glycine, post-synaptic depolarization occurs, leading to the removal of a Mg²⁺ channel block, allowing the influx of Na⁺ and Ca²⁺ ions into the postsynaptic cell. This overall process leads to glutamate signal transduction from a pre- to a post-synaptic cell.

In recent years, several central nervous system disorders have been associated with misregulation and overstimulation of the NMDAR, such as ischemia,² epilepsy³ and pain amplification.⁴ Various neurodegenerative disorders have also been linked to defective NMDA pathways, such as Parkinson's and Alzheimer's diseases and even neuropsychiatric disorders, such as schizophrenia.^{5,6} In seeking to combat these effects, selective

NMDAR antagonists have been considered as potential therapeutic and diagnostic agents.^{7,8}

Magnetic Resonance Imaging (MRI) is regarded as one of the most powerful, non-invasive diagnostic imaging techniques used in clinical and biomedical research. The sensitivity and specificity, and hence contrast of MR images, can be further enhanced by the use of responsive contrast agents. Notwithstanding numerous *in vivo* techniques available to neuroscientists, our current understanding of the dynamic changes and molecular basis of neural activity is far from complete. Therefore, by employing a targeted, responsive contrast agent that can report changes in neural activity non-invasively, MRI could provide new vital information on these important homeostatic processes.

One suggested way is through the use of selective glutamate-receptor contrast agents, which can bind selectively to the NMDAR and with sufficient affinity to act as a marker of receptor density. For such a system to be responsive, stimulated release of glutamate from the pre-synaptic cell, which takes place over a duration of milliseconds, should displace the contrast agent from the NMDAR, whilst restoration of the equilibrium state is believed to occur over a period of about a second.⁹

Caravan has proposed¹⁰ that in order to observe a 10% increase in the observed water proton relaxation rate, R_1 , by using a contrast agent with relaxivity of 5 mM⁻¹ s⁻¹, a 10 μM local concentration of the Gd-agent is needed. This corresponds to 10⁷ Gd-chelates per cell, suggesting that this is the required NMDAR density needed to observe a change in contrast. At present, there is no typical value reported for the NMDAR density; values have been reported to be as high as 6.4 pm mg⁻¹.¹¹ However, Sherry *et al.* have reported¹² that even if the bulk receptor density is low, the receptors can still be imaged successfully at less than 10 μM local concentrations, if the receptors cluster together and form micro-domains of high local concentration. Furthermore, the rate of dissociation of the contrast agent from the receptor may

^aDepartment of Chemistry, Durham University, South Road, Durham, DH1 3LE, England. E-mail: anurag.mishra@durham.ac.uk; david.parker@durham.ac.uk; Fax: +44-191-3342051

^bHigh Field MR Centre, Max Planck Institute for Biological Cybernetics, Spemannstrasse 41, Tuebingen, 72076, Germany

† Electronic supplementary information (ESI) available (37 pages): Synthetic procedures, microscopy and spectral imaging instrumentation and operating procedures, cell culture, toxicity and MR experiments. See DOI: 10.1039/c3sc50903f

‡ Present address: Institute for Biological and Medical Imaging, Helmholtz Center Munich, Neuherberg, Germany.

be slow. If the affinity of the targeted contrast agent is of the order of $\log K_a = 7.0$, then if the rate of association is 10^6 – 10^7 Hz, the dissociation rate will be of the order of 0.1–1 Hz. Therefore, the timescale of the imaging experiment is likely to be the same order of magnitude as the lifetime of the receptor bound complex, potentially increasing the intrinsic sensitivity of the experiment. Assuming that local concentrations of the contrast agent do not change within this timescale, it should be possible to report these changes by modulation of the water proton relaxivity, reflecting the relative amounts of receptor bound and unbound contrast agent.

Here, we report the design, synthesis and *in vitro* evaluation of a series of NMDA receptor-targeted contrast agents. The contrast agents are based on well-known competitive NMDAR antagonists, appended to an *N*-linked 'Gd-DOTA' core that possesses a fast-exchanging water molecule. The proposed contrast agents focus on modulation of the rotational correlation time, τ_R . In the low to medium field range (3–7 T), this term dominates the water proton relaxivity for a low molecular weight complex, when water exchange at the metal centre is relatively fast.¹³ The contrast agents have been designed so that in the bound state, molecular tumbling is slower than in the unbound state. This increases the τ_R value, giving a significant relaxivity change, represented as a modulation of R_1 ($R_1 = 1/T_1$).

Results and discussion

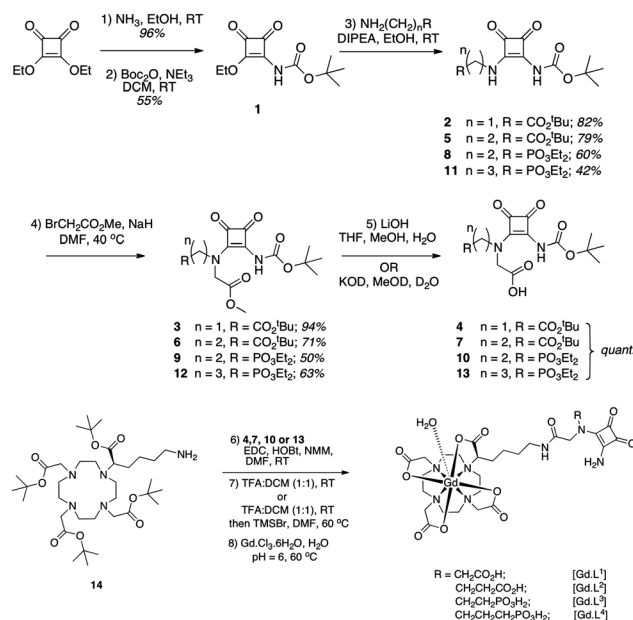
Ligand design and complex synthesis

Several competitive NMDAR antagonists have been reported that contain the α -amino carboxylic acid and phosphonic acid functionalities, separated by a carbon spacer unit.^{7,14} The 3,4-diamino-3-cyclobutene-1,2-dione moiety acts as an isostere for the α -amino carboxylic acid functionality, and has been incorporated into functional NMDA antagonists.¹⁴ The synthesis of the NMDA receptor-targeted contrast agents is detailed in Scheme 1. Monoamination followed by BOC protection of 3,4-diethoxy-3-cyclobutene-1,2-dione gave the intermediate **1**. A Michael-type addition–elimination reaction using commercially available glycine/ β -alanine *tert*-butyl ester, diethyl(2-aminoethyl)phosphonate, or diethyl(3-aminopropyl)phosphonate¹⁵ yielded compounds **2**, **5**, **8** and **11**, respectively. Subsequent *N*-alkylation with methyl bromoacetate in the presence of base gave the fully protected antagonist entities, **3**, **6**, **9** and **12**. Finally, selective ester hydrolysis, under ambient basic conditions, gave compounds **4**, **7**, **10** and **13** in quantitative yield.

The antagonist fragments were coupled through the carboxylic acid to the macrocyclic amine, **14**, (ESI⁺) using standard amide-coupling techniques, (EDC/HOBt/MMM) in anhydrous DMF, to give the fully protected ligands, which were hydrolyzed under acidic conditions. Complexation was achieved using $\text{GdCl}_3 \cdot 6\text{H}_2\text{O}$ in water at pH 6 and 60 °C, to give the complexes $[\text{Gd.L}^{1-4}]$.

Relaxivity properties

The total gadolinium concentration of $[\text{Gd.L}^{1-4}]$ was measured using Evans' bulk magnetic susceptibility measurements.¹⁶ The



Scheme 1 Synthesis of NMDA-targeted contrast agents, $[\text{Gd.L}^{1-4}]$.

longitudinal proton relaxivity of $[\text{Gd.L}^{1-4}]$ was measured in aqueous solution (pH 7.4) at 37 °C and 1.4 T. The relaxivities for $[\text{Gd.L}^{1-4}]$ were 5.17, 5.30, 4.68 and 4.80 $\text{mM}^{-1} \text{s}^{-1}$, respectively. Such values lie in the expected range for mono-aqua gadolinium species of this molecular weight.¹⁷

Human Serum Albumin (HSA) is a globular protein constituting around 4.5% of plasma. As it is the major protein constituent in the circulatory system, it is likely that the contrast agent will bind to the protein, disrupting its rotational dynamics leading to an enhancement of the longitudinal relaxation rate of the water protons. Therefore, as a control experiment, the effect of HSA on the measured relaxivity of $[\text{Gd.L}^{1-4}]$ (each at 1 mM) was assessed at 1.4 T in the presence of up to 1.6 mM HSA. This led to an increase in r_{1p} of 54%, 193%, 39% and 66% for $[\text{Gd.L}^{1-4}]$, respectively (ESI[†]). Association constants were estimated assuming a 1 : 1 stoichiometry of interaction, and were found to be $\log K_a = 3.50(\pm 0.03)$ and $\log K_a = 3.90(\pm 0.02)$ for the carboxylate analogues $[\text{Gd.L}^{1,2}]$, and $\log K_a = 2.50(\pm 0.03)$ and $3.05(\pm 0.02)$ for the phosphonate analogues $[\text{Gd.L}^{3,4}]$ (Table 1).

Table 1 Binding affinities to serum albumin,^{a,b,c} and relaxation properties of the complexes reported herein (310 K, pH 7.4, 1.4 T)

	$[\text{Gd.L}^1]$	$[\text{Gd.L}^2]$	$[\text{Gd.L}^3]$	$[\text{Gd.L}^4]$
$\log K_a$	3.50 ^a	3.90 ^b	2.50 ^a	3.05 ^b
$r_{1p}^{\text{initial}}/\text{mM}^{-1} \text{s}^{-1}$	5.17	5.30	4.68	4.80
r_{1p} at 0.7 mM HSA/ $\text{mM}^{-1} \text{s}^{-1}$	7.62	11.44	5.57	6.70
$r_{1p}^{\text{limit}}/\text{mM}^{-1} \text{s}^{-1}$	11	18	14	11

^a Error is $\pm 0.03 \text{ mM}^{-1} \text{s}^{-1}$. ^b Error is $\pm 0.02 \text{ mM}^{-1} \text{s}^{-1}$. ^c The reported relative affinities for the NMDA binding moiety in L^{1-4} are 2.3, 1.6, 0.47 and 2.6 μM respectively; these were given as IC_{50} values, *i.e.* they are not the 1 : 1 binding constants.¹⁴

By comparing each pair (carboxylic acid vs. phosphonic acid), it is apparent that increasing the chain length of the pendant acidic arm promotes the binding interaction between the complex and the protein. In the case of $[\text{Gd.L}^2]$, a much larger percentage increase in r_{1p} was observed compared to any other complex. Such behaviour is consistent with a stronger complex–protein interaction, modulating τ_R more significantly.

Probe-receptor binding studies

A neuronal cell line model expressing functional NMDA receptors was established using the NSC-34 cell line. This hybrid cell-line is produced by the fusion of mouse spinal cord and neuroblastoma cells and has been used previously for the evaluation of NMDAR antagonists.¹⁸

The expression of NMDAR on differentiated NSC-34 cells was demonstrated using immunofluorescence techniques with different primary antibodies; one for each of the two subunits NMDAR-1 and NMDAR-2B of the receptor, thus demonstrating the expression of functional receptors (ESI†).

Cellular labelling of differentiated NSC-34 cells with $[\text{Gd.L}^{1-4}]$ was assessed by measuring the longitudinal relaxation times, T_1 , of the cells on a 3 T Siemens human whole body MR scanner equipped with a head coil, allowing the calculation of cellular relaxation rates, $R_{1,\text{cell}}$. Differentiated cells were incubated (37 °C, 5% CO_2) for 45 min with 200 μM $[\text{Gd.L}^{1-4}]$, washed with Hank's Buffered Saline Solution (HBSS) to remove any unbound complex, re-suspended in fresh buffer and T_1 -weighted MR images were acquired (Fig. 1 and ESI†).

The complexes $[\text{Gd.L}^{1-4}]$ each contain the 3,4-diamino-3-cyclobutene-1,2-dione moiety, that serves as an isosteric replacement of the α -amino carboxylic acid functionality known to be essential for many of the reported competitive NMDAR antagonists.⁷ The complexes $[\text{Gd.L}^{1,2}]$ incorporate a carboxylic acid residue of variable chain length (1 or 2) appended to one of the α -amines. Although $[\text{Gd.L}^1]$ exhibits an increase in $R_{1,\text{cell}}$ (118% of control), the homologue, $[\text{Gd.L}^2]$, with increased pendant chain length ($n = 2$) displays a statistically higher increase in $R_{1,\text{cell}}$ (170% of control). This result is in keeping with the trend in affinity constants for the antagonist moieties.¹⁴

It was hypothesised that the phosphonic acid derivatives, $[\text{Gd.L}^{3,4}]$ would bind more strongly to the NMDAR, leading to a larger increase in $R_{1,\text{cell}}$. Interestingly, $[\text{Gd.L}^3]$ showed no apparent receptor specific binding, despite the antagonist portion being reported to be particularly potent.¹⁴ We have previously shown¹⁹ that appending the sterically demanding macrocyclic core to a known antagonist can alter the antagonists' affinity for a receptor, and this could be an explanation of the lack of binding for $[\text{Gd.L}^3]$. However, a more likely argument is that rotameric forms of $[\text{Gd.L}^3]$ exist, arising from rotation around the C–N bond of the squaramide moiety in which intramolecular H-bonding gives rise to relatively stable 8/9-ring chelates. This intramolecular H-bonding interaction may weaken the binding of the antagonist towards the NMDAR (Scheme 2).²⁰

In contrast, $[\text{Gd.L}^4]$ with a longer 3 carbon spacer, adopts a geometry in which binding to the NMDAR is not perturbed so

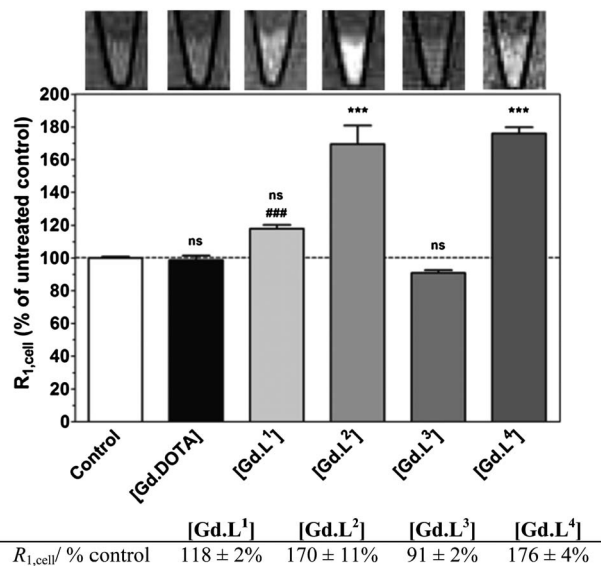
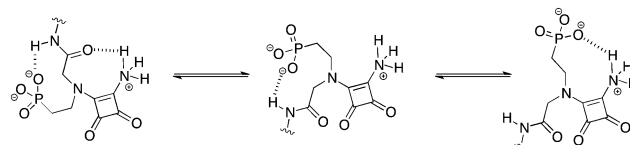


Fig. 1 (Top) Representative T_1 -weighted MR-images of 1×10^7 untreated differentiated cells (control) and differentiated cells treated for 45 min with 200 μM of $[\text{Gd.DOTA}]$ or $[\text{Gd.L}^{1-4}]$. Images were recorded using a turbo spin echo sequence with a matrix of 256×256 voxels over a field of view of $110 \times 110 \text{ mm}^2$, slice thickness of 1 mm (resulting in a voxel size of $0.4 \times 0.4 \times 1.0 \text{ mm}^3$), T_R 1000 ms, T_E 13 ms, T_i 23 ms and 20 averages; (bottom) cellular ^1H MR relaxation rates $R_{1,\text{cell}}$ in cell suspensions (3 T, 298 K) after treatment of differentiated NSC-34 cells with 200 μM $[\text{Gd.DOTA}]$ or $[\text{Gd.L}^{1-4}]$ for 45 min. $[\text{Gd.DOTA}]$ served as a negative control. Values are mean \pm SEM ($n = 3-6$). ns: not significant, $***P < 0.001$ ANOVA with Bonferroni's multiple comparison post-test. $###P < 0.001$ Student's t -test. Both tests vs. untreated control using Graphpad Prism 5.02.



Scheme 2 Possible rotameric forms of $[\text{Gd.L}^3]$ due to intramolecular hydrogen bonding.

much. It gave rise to the largest observed increase in $R_{1,\text{cell}}$ (176% of control).

It is thought that for an MRI experiment of this nature to be viable at least 3×10^7 bound Gd-complexes per cell are required.²¹ By using Gd-ICP-MS (data from Fig. 1), the average number of $[\text{Gd.L}^4]$ complexes per cell was determined, that resulted in the measured change in $R_{1,\text{cell}}$. Using this technique, 9.3×10^8 Gd^{3+} ions per cell were estimated, revealing an estimated local Gd^{3+} concentration of 370 μM . This value is beyond the theoretical detection limit, and explains the large enhancement in cellular relaxation rate observed.

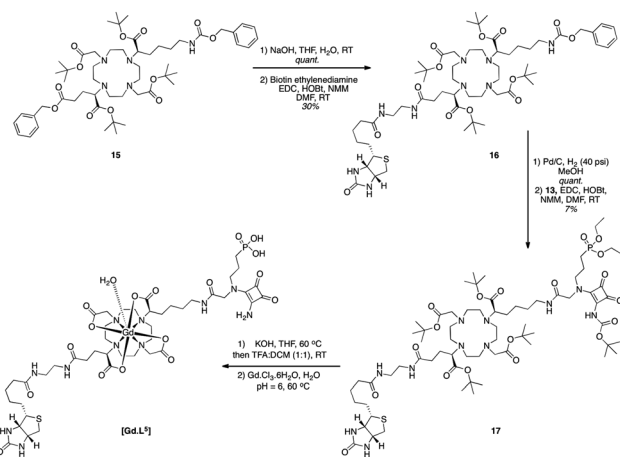
The cytotoxicity of the four gadolinium complexes $[\text{Gd.L}^{1-4}]$ was studied by assessing the metabolic activity of differentiated NSC-34 cells using an MTT assay.²² None of the complexes exhibited any cytotoxic effects at concentrations of up to 200 μM , following a 24 hour incubation (ESI†).

Cell-surface immobilisation and visualisation of NMDA receptors

The variation of $R_{1,\text{cell}}$ in the presence of $[\text{Gd.L}^2]$ and $[\text{Gd.L}^4]$ is consistent with an increase in τ_R that is associated with slower molecular tumbling of the complex when bound to the cell surface receptors. However, internalisation of the complex *via* receptor-mediated endocytosis or non-specific binding to the cell membrane are also possible mechanisms that could lead to an increase in $R_{1,\text{cell}}$. In order to establish which of these possibilities is responsible for the observed increase in $R_{1,\text{cell}}$, a new complex was designed that allows direct visualisation of the contrast agent on the cell surface.

Appending a fluorescent label to a non-competitive antagonist has recently been shown to allow for the direct visualisation of the NMDAR-2B subunit.²³ However, we^{24–27} and Barton and Puckett^{28,29} have shown that some fluorescent labels perturb cell-uptake mechanisms and may promote internalisation of the complex. Therefore, $[\text{Gd.L}^5]$ was designed, comprising the antagonist binding portion of the most promising contrast agent, $[\text{Gd.L}^4]$ (largest increase in $R_{1,\text{cell}}$), in which a *trans*-substituted biotin moiety is appended to the macrocyclic core. It was envisaged that if cell-surface receptor binding is responsible for the increase in $R_{1,\text{cell}}$ for $[\text{Gd.L}^{2/4}]$, the biotin moiety of $[\text{Gd.L}^5]$, after binding to an added AvidinAlexaFluor® 488 conjugate, would act as a tag on the outside of the cell, allowing direct visualisation of the complex only when it is bound to the cell surface.

The synthesis of $[\text{Gd.L}^5]$ (Scheme 3) involves standard protection and deprotection steps (ESI^+). Following modification of the dicarboxymethyl cyclen precursor, the benzyl group of **15** was selectively removed to allow conjugation of the pre-formed biotin ethylenediamine. Removal of the Cbz group from the *N*-terminus of the pendant lysine arm on **16** allowed for coupling of the antagonist moiety to give **17**, as described in the synthesis of $[\text{Gd.L}^4]$. Finally, after selective basic and acidic hydrolysis of the protecting groups, gadolinium was introduced to give the complex $[\text{Gd.L}^5]$, with a relaxivity of $7.24 \text{ mM}^{-1} \text{ s}^{-1}$,



Scheme 3 Synthesis of the bifunctional MR imaging probe, $[\text{Gd.L}^5]$, in which a biotin moiety is included, spaced from the NMDA-receptor binding sub-unit.

measured at pH 7.4, 37 °C and 60 MHz (1.4 T). The increased relaxivity is associated with the larger molecular volume of the complex, giving rise to a slower rotational correlation time. Also, an increased second sphere hydration may occur with this complex, through multiple hydrogen bonding interactions.³⁰

In order to study the behaviour and localisation of $[\text{Gd.L}^5]$, live-cell laser scanning confocal microscopy (LSCM) imaging studies were carried out. Differentiated NSC-34 cells were grown on a specially designed microscope slide comprising of a flow-through channel (100 μL) and subjected to various conditions. Simultaneous treatment with a solution of $[\text{Gd.L}^5]$ (10 μM) and AvidinAlexaFluor® 488 conjugate (2.5 μM , 10 min) showed a localization profile, resembling pit-like localization at the cell surface (Fig. 2A). CellMask™ Orange is a commercially available dye for non-specific staining of the plasma membrane. A repeat of the simultaneous loading experiment of $[\text{Gd.L}^5]$ and AvidinAlexaFluor® 488 conjugate (10 min), co-incubated with a CellMask™ Orange (5 min, 5 $\mu\text{g mL}^{-1}$), showed unequivocal evidence for the selective localisation of $[\text{Gd.L}^5]$ at the cell membrane (Fig. 2B/C).

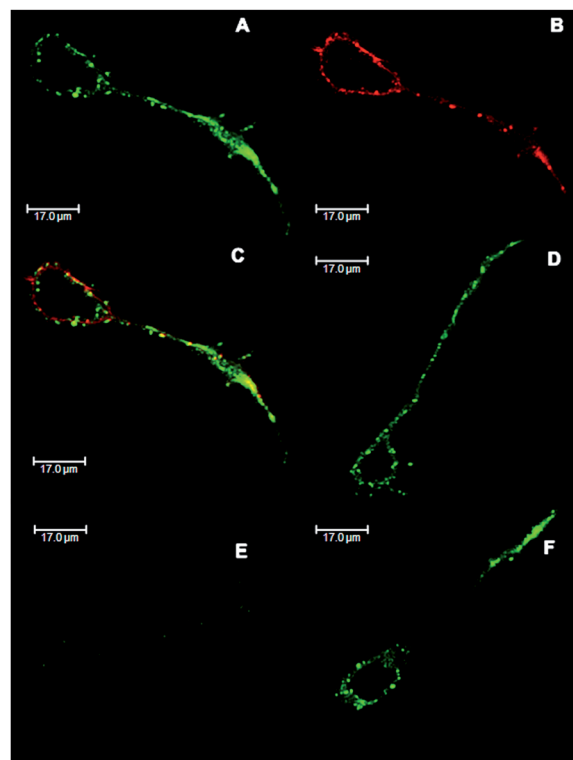


Fig. 2 Live cell LSCM images of differentiated NSC-34 cells following treatment with $[\text{Gd.L}^5]$. (A) Simultaneous loading of $[\text{Gd.L}^5]$ (10 μM), and AvidinAlexaFluor® 488 conjugate (2.5 μM , 10 min) allowing visualisation of AvidinAlexaFluor® 488 conjugate $\lambda_{\text{ex}}/\lambda_{\text{em}} = 488/505\text{--}555 \text{ nm}$; (B) As (A) but with a 5 minute CellMask™ Orange incubation allowing visualisation of CellMask™ Orange $\lambda_{\text{ex}}/\lambda_{\text{em}} = 543/550\text{--}660 \text{ nm}$; (C) RGB merge showing co-localisation of the AvidinAlexaFluor® 488 conjugate and CellMask™ Orange on the cell surface ($P = 0.88$); (D) As image (A); (E) As image (A) but with a post-glutamate (1 mM) wash showing that $[\text{Gd.L}^5]$ is removed from cell surface and; (F) NSC-34 cells are treated with glutamate (1 mM) and then simultaneous loading of $[\text{Gd.L}^5]$ (10 μM), and AvidinAlexaFluor® 488 conjugate (2.5 μM , 10 min) allows recovery of 35% of the fluorescence signal intensity as compared to image (A).

Confirmation that the observed fluorescence was due to the strong ($\log K_a > 15$) biotin–avidin interaction between $[\text{Gd.L}^5]$ and AvidinAlexaFluor® 488 conjugate, was demonstrated in two control experiments. Differentiated, untreated NSC-34 cells (ESI Fig. S3†) and differentiated cells loaded with AvidinAlexaFluor® 488 conjugate only (ESI Fig. S3†), showed no observable fluorescence signal in the visible region of the spectrum, when using the previously established experimental parameters. Cell surface localisation was found to be independent of the loading concentration (up to 100 μM) and time (up to 45 minutes) and did not vary for stepwise *vs.* simultaneous incubations of the donor and acceptor (data not shown). No evidence for any intracellular staining was observed throughout these experiments; further evidence of cell-surface localisation has been derived from a 3D reconstruction (ESI: video†) of the LSCM images taken following simultaneous incubation of $[\text{Gd.L}^5]$ (10 μM) and the AvidinAlexaFluor® 488 conjugate (2.5 μM , 10 min).

Establishing the specificity and reversibility of binding

The two key characteristics needed for a probe of this nature are specificity and reversibility. Evidence for the first of these was obtained following simultaneous incubation of an NMDA receptor-negative cell line, NIH-3T3, with $[\text{Gd.L}^5]$ (10 μM) and AvidinAlexaFluor® 488 conjugate (2.5 μM , 10 min). No localisation of any kind (cell surface or intracellular) was observed, strengthening the argument of a receptor-mediated effect, only in the NSC-34 cells (ESI: Fig. S4†).

The reversibility of $[\text{Gd.L}^5]$ receptor binding was also demonstrated through a glutamate/aspartate washing experiment. As before, differentiated NSC-34 cells underwent simultaneous incubation with a solution of $[\text{Gd.L}^5]$ (10 μM) and AvidinAlexaFluor® 488 conjugate (2.5 μM , 10 min) (Fig. 2D). By washing the cells with 5 successive aliquots ($V_{\text{tot}} = 500 \mu\text{L}$) of a glutamate rich (1 mM) culture medium, a ten-fold drop in fluorescence intensity was observed, compared to the original cell staining experiment (Fig. 2E). Furthermore, by substituting glutamate in the wash solution with the weaker natural agonist, aspartate (5 aliquots of 1 mM), only 38% of the original intensity was observed (ESI Fig. S6†).

The ability of the probe to displace glutamate was also demonstrated. When differentiated NSC-34 cells were sequentially treated with five volumetric aliquots of a glutamate rich (1 mM) culture medium, then washed with normal culture media and finally incubated with a solution of $[\text{Gd.L}^5]$ (10 μM) and AvidinAlexaFluor® 488 conjugate (2.5 μM , 10 min), a 35% fluorescence recovery was observed, compared to the original cell staining experiment (Fig. 2F). Such behaviour demonstrates the capability of $[\text{Gd.L}^5]$ to displace glutamate from the receptor-binding site, for example after a glutamate burst.

Taken together these results indicate that $[\text{Gd.L}^5]$ binds to the cell surface glutamate-binding site of the NMDAR, *via* the antagonist squaramide moiety.

Conclusions

In summary, a series of MR imaging probes targeted to the NMDAR has been created, using an antagonist-receptor

mediated targeting approach. The most promising contrast agent, $[\text{Gd.L}^4]$, showed a 176% increase in relaxation rate in the presence of functional NMDARs on differentiated NSC-34 cells. Cell-surface localisation was demonstrated for the derivative, $[\text{Gd.L}^5]$, providing evidence for specificity, as no binding was observed upon incubation with an NMDA receptor negative cell-line.

The reversibility of the binding of the contrast agent to the receptors was also demonstrated. Addition of glutamate to the receptor-bound $[\text{Gd.L}^5]$ led to displacement of the complex from the receptors, resulting in a diminution of signal intensity, which was partially recovered upon subsequent incubation with $[\text{Gd.L}^5]$ and the AvidinAlexaFluor® 488 conjugate.

This work suggests that the gadolinium complexes of L^2 and L^4 are promising MR contrast agent candidates for reporting or monitoring NMDAR density and have the potential to report on synaptic glutamate activity. It is appreciated that for use *in vivo*, direct intra-cranial injection or artificially altering the permeability of the blood–brain barrier (BBB) are required for such anionic complexes to enter the brain. Therefore, future work will attempt to seek to extend these encouraging *in vitro* results, by following changes in the MR signal intensity in an appropriate animal model. In parallel, more potent antagonist-conjugate systems will be examined, in which the binding constants of the antagonist are even higher.

Acknowledgements

We thank the EPSRC and the ERC (FCC266804) for support.

Notes and references

- 1 S. F. Traynelis, L. P. Wollmuth, C. J. McBain, F. S. Menniti, K. M. Vance, K. K. Ogden, K. B. Hansen, H. J. Yuan, S. J. Myers and R. Dingledine, *Pharmacol. Rev.*, 2010, **62**, 405–496.
- 2 L. Mony, J. N. C. Kew, M. J. Gunthorpe and P. Paoletti, *Br. J. Pharmacol.*, 2009, **157**, 1301–1317.
- 3 G. J. Lees, *Neuroscience*, 1993, **54**, 287–322.
- 4 A. B. Petrenko, T. Yamakura, A. Baba and K. Shimoji, *Anesthesia and Analgesia*, 2003, **97**, 1108–1116.
- 5 S. Cull-Candy, S. Brickley and M. Farrant, *Curr. Opin. Neurobiol.*, 2001, **11**, 327–335.
- 6 E. A. Waxman and D. R. Lynch, *Neuroscientist*, 2005, **11**, 37–49.
- 7 H. Bräuner-Osborne, J. Egebjerg, E. Ø. Nielsen, U. Madsen and P. Krosgaard-Larsen, *J. Med. Chem.*, 2000, **43**, 2609–2645.
- 8 W. E. Childers and R. B. Baudy, *J. Med. Chem.*, 2007, **50**, 2557–2562.
- 9 S. A. Hires, Y. Zhu and R. Y. Tsien, *Proc. Natl. Acad. Sci. U. S. A.*, 2008, **105**, 4411–4416.
- 10 P. Caravan and Z. Zhang, *Eur. J. Inorg. Chem.*, 2012, 1916–1923.
- 11 D. E. Murphy, J. Schneider, C. Boehm, J. Lehmann and M. Williams, *J. Pharmacol. Exp. Ther.*, 1987, **240**, 778–784.

- 12 K. Hanaoka, A. J. M. Lubag, A. Castillo-Muzquiz, T. Kodadek and A. D. Sherry, *Magn. Reson. Imaging*, 2008, **26**, 608–617.
- 13 R. B. Lauffer, *Chem. Rev.*, 1987, **87**, 901–927.
- 14 W. A. Kinney, N. E. Lee, D. T. Garrison, E. J. Podlesny, J. T. Simmonds, D. Bramlett, R. R. Notvest, D. M. Kowal and R. P. Tasse, *J. Med. Chem.*, 1992, **35**, 4720–4726.
- 15 P. Bakó, T. Novák, K. Ludányi, B. Pete, T. László and G. Keglevich, *Tetrahedron: Asymmetry*, 1999, **10**, 2373–2380.
- 16 D. M. Corsi, C. Platas-Iglesias, H. van Bekkum and J. A. Peters, *Magn. Reson. Chem.*, 2001, **39**, 723–726.
- 17 A. E. Merbach, *The Chemistry of Contrast Agents in Medical Magnetic Resonance Imaging*, ed. A. E. Merbach and É. Tóth, Wiley, New York, Chichester, 2001.
- 18 C. J. Eggett, S. Crosier, P. Manning, M. R. Cookson, F. M. Menzies, C. J. McNeil and P. J. Shaw, *J. Neurochem.*, 2000, **74**, 1895–1902.
- 19 A. Mishra, S. Gottschalk, J. Engelmann and D. Parker, *Chem. Sci.*, 2012, **3**, 131–135.
- 20 W. A. Kinney, M. Abou-Gharbia, D. T. Garrison, J. Schmid, D. M. Kowal, D. R. Bramlett, T. L. Miller, R. P. Tasse, M. M. Zaleska and J. A. Moyer, *J. Med. Chem.*, 1998, **41**, 236–246.
- 21 S. Aime, C. Cabella, S. Colombatto, S. Geninatti Crich, E. Gianolio and F. Maggioni, *J. Magn. Reson. Imaging*, 2002, **16**, 394–406.
- 22 J. Carmichael, W. G. Degraff, A. F. Gazdar, J. D. Minna and J. B. Mitchell, *Cancer Res.*, 1987, **47**, 936–942.
- 23 P. Marchand, J. Becerril-Ortega, L. Mony, C. Bouteiller, P. Paoletti, O. Nicole, L. Barré, A. Buisson and C. Perrio, *Bioconjugate Chem.*, 2011, **23**, 21–26.
- 24 F. Kielar, A. Congreve, G.-l. Law, E. J. New, D. Parker, K.-L. Wong, P. Castreno and J. de Mendoza, *Chem. Commun.*, 2008, 2435–2437.
- 25 C. P. Montgomery, B. S. Murray, E. J. New, R. Pal and D. Parker, *Acc. Chem. Res.*, 2009, **42**, 925–937.
- 26 E. J. New, D. Parker and R. D. Peacock, *Dalton Trans.*, 2009, 672–679.
- 27 E. J. New, A. Congreve and D. Parker, *Chem. Sci.*, 2010, **1**, 111–118.
- 28 C. A. Puckett and J. K. Barton, *Biochemistry*, 2008, **47**, 11711–11716.
- 29 C. A. Puckett and J. K. Barton, *J. Am. Chem. Soc.*, 2009, **131**, 8738–8739.
- 30 M. Botta, *Eur. J. Inorg. Chem.*, 2000, 399–407.